ACCOUNTS of chemical research

Article

pubs.acs.org/accounts

Amorphous Molybdenum Sulfides as Hydrogen Evolution Catalysts

Carlos G. Morales-Guio and Xile Hu*

Laboratory of Inorganic Synthesis and Catalysis, Institute of Chemical Sciences and Engineering, École Polytechnique Fédérale de Lausanne (EPFL), BCH 3305, Lausanne 1015, Switzerland

CONSPECTUS: Providing energy for a population projected to reach 9 billion people within the middle of this century is one of the most pressing societal issues. Burning fossil fuels at a rate and scale that satisfy our near-term demand will irreversibly damage the living environment. Among the various sources of alternative and CO_2-emission-free energies, the sun is the only source that is capable of providing enough energy for the whole world. Sunlight energy, however, is intermittent and requires an efficient storage mechanism. Sunlight-driven water splitting to make hydrogen is widely considered as one of the most attractive methods for solar energy storage. Water splitting needs a hydrogen evolution catalyst to accelerate the rate of hydrogen production and to lower the energy loss in this process. Precious metals such as Pt are superior catalysts, but they are too expensive and scarce for large-scale applications.

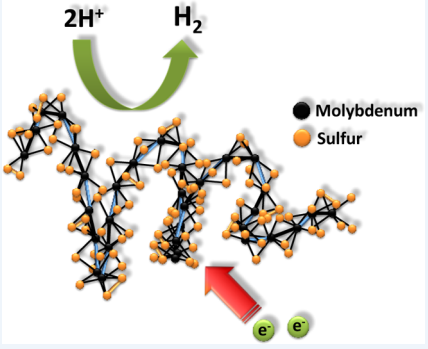

In this Account, we summarize our recent research on the preparation, characterization, and application of amorphous molybdenum sulfide catalysts for the hydrogen evolution reaction. The catalysts can be synthesized by electrochemical deposition under ambient conditions from readily available and inexpensive precursors. The catalytic activity is among the highest for nonprecious catalysts. For example, at a loading of 0.2 mg/cm^2, the optimal catalyst delivers a current density of 10 mA/cm^2 at an overpotential of 160 mV. The growth mechanism of the electrochemically deposited film catalysts was revealed by an electrochemical quartz microcrystal balance study. While different electrochemical deposition methods produce films with different initial compositions, the active catalysts are the same and are identified as a "MoS_{2+x}" species. The activity of the film catalysts can be further promoted by divalent Fe, Co, and Ni ions, and the origins of the promotional effects have been probed. Highly active amorphous molybdenum sulfide particles can also be prepared from simple wet-chemical routes. Electron transport is sometimes slow in the particle catalysts, and an impedance model has been established to identify this slow electron transport. Finally, the amorphous molybdenum sulfide film catalyst has been integrated onto a copper(I) oxide photocathode for photoelectrochemical hydrogen evolution. The conformal catalyst efficiently extracts the excited electrons to give an impressive photocurrent density of −5.7 mA/cm^2 at 0 V vs RHE. The catalyst also confers good stability.

INTRODUCTION

Solar irradiation reaching the surface of the Earth in a period of 1 h is sufficient to satisfy the world's energy demand for one whole year at the current consumption rate.[1] However, solar energy harvesting is often separated in time and location from consumption, demanding efficient energy storage and distribution systems at a scale commensurate with our energy demand. Electrochemical and photoelectrochemical production of hydrogen from water has long been considered as an attractive method for solar energy storage.[2,3] Hydrogen is a clean energy vector that can be stored, distributed, and used on demand and generates clean water as exhaust.[4] Pt-group metals are the most efficient electrocatalysts for the hydrogen evolution reaction (HER), $2H^+ + 2e^- \rightarrow H_2$. Unfortunately, these metals are among the rarest and most expensive elements on earth, making them unsuitable for energy storage on a global scale. Therefore, it is imperative to replace Pt-group metals with materials made entirely of earth-abundant elements for the HER. In addition, technoeconomic analyses have suggested that a lifetime of 15 or better 20 years for a solar hydrogen production device is required in order to achieve economically competitive H_2 production.[5] This requirement further limits HER catalysts only to those of superior stability, simple maintenance, and minimum environmental impact during operation and at the end of the use life.[6]

Hinnemann et al.[7] identified the edge site of MoS_2 as a promising hydrogen evolution catalyst in 2005. In principle, when the free energy of adsorbed atomic hydrogen is close to that of the reactant or product (i.e., $\Delta G^\circ_H \approx 0$), a material is potentially a good HER catalyst.[8] They showed by density functional theory (DFT) calculations that this holds for the active sites of hydrogen-evolving enzymes such as nitrogenase and hydrogenase and the edge site of MoS_2. Subsequent experiments by Jaramillo et al.[9] using MoS_2 nanocrystals showed that the HER activity is indeed directly proportional to the edge length of the crystals but not to the surface area. Preferential exposure of edge sites has resulted in more active MoS_2 electrocatalysts.[10,11] Since the original studies of Hinneman et al. and Jaramillo et al., extensive efforts have

Received: May 23, 2014
Published: July 28, 2014

   dx.doi.org/10.1021/ar5002022 | Acc. Chem. Res. 2014, 47, 2671−2681

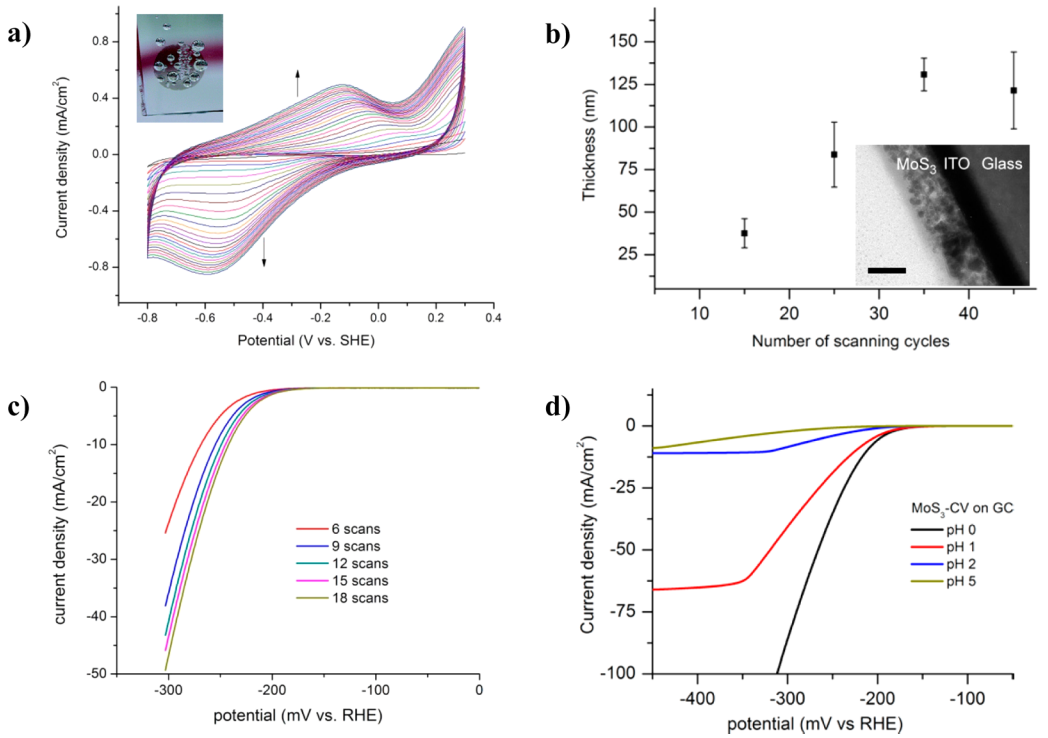

Figure 1. (a) Cyclic voltammograms during the deposition of a molybdenum sulfide film by cyclic voltammetry (25 cycles). Conditions: glassy carbon substrate, $NaClO_4$ electrolyte (0.1 M), 2 mM $(NH_4)_2[MoS_4]$, scan rate = 50 mV/s. Inset: digital image of an amorphous molybdenum sulfide film on ITO during hydrogen evolution. (b) Thickness of MoS_3-CV films as a function of the number of scanning cycles. Inset: SEM image of a MoS_3-CV film on ITO. The scale bar corresponds to 50 nm. (c) Polarization curves (at pH 0) of MoS_3-CV films made from different numbers of scanning cycles. The films were deposited on a rotating glassy carbon electrode. (d) Polarization curves of a MoS_3-CV film on a rotating glassy carbon disk electrode recorded at different pHs. Adapted with permission from ref 18. Copyright 2011 Royal Society of Chemistry.

been devoted to the preparation of nanostructured crystalline molybdenum sulfide materials for the HER; these efforts have been reviewed by us and others.[12−15] This Account deals with a related but different type of material: amorphous molybdenum sulfides.

Amorphous molybdenum sulfides have proved to be highly active and versatile catalysts for the HER in acidic solutions. Amorphous materials are generally prepared at milder temperatures and with faster solidification processes than crystalline materials. Although amorphous molybdenum sulfides lack long-range order, they have short-range atomic arrangements[16,17] that give rise to interesting catalytic properties. Our group discovered that amorphous molybdenum sulfides, which have been known since 1825, are a highly active catalyst for the HER.[18] The simple and mild preparation methods along with the low cost of the precursor materials make this class of catalysts very attractive for the development of cost-effective electrochemical and photoelectrochemical hydrogen production devices. This Account summarizes our work from the first report in 2011 up to a recent application in photoelectrochemical hydrogen production.

DISCOVERY OF AMORPHOUS MOLYBDENUM SULFIDE FILMS AS HER CATALYSTS

Sometime in 2009, we considered $[MoS_4]^{2-}$ and its transition-metal complexes $[M(MoS_4)_2]^{2-}$ as potential homogeneous HER catalysts. These compounds contain only sulfur ligands, which are ubiquitous in the active sites of hydrogenase and nitrogenase enzymes. Additionally, they are either commercially available or easy to synthesize. We quickly found that hydrogen evolution occurs from solutions containing these compounds, but more thorough investigations revealed that the molecular complexes decompose under the electrolysis conditions to yield active heterogeneous catalysts on the electrodes.[19] This initiated our research on the preparation and application of these catalysts, later identified as amorphous molybdenum sulfides.

The initially optimized deposition method for amorphous molybdenum sulfide was cyclic voltammetry (CV). In a typical potential cycling experiment conducted for an aqueous solution of $[MoS_4]^{2-}$, one reduction peak and one oxidation peak grew at −0.2 and 0.3 V versus the reversible hydrogen electrode (RHE), respectively (Figure 1a); at the same time, a brownish film started to form on the electrode.[18] The deposition worked on various conductive substrates such as fluorine-doped tin oxide (FTO), indium tin oxide (ITO), and glassy carbon (GC) electrodes. The thickness of the electrodeposited films increased with the number of scanning cycles up to a few hundred nanometers (Figure 1b). The current density for the HER increased when the number of scanning cycles during deposition was increased, indicating a porous nature of the catalyst film (Figure 1c).

The HER catalytic activity of these molybdenum sulfide films, initially labeled as MoS_x-CV, was first studied by linear sweep voltammetry. Figure 1d shows the polarization curves of MoS_3-CV on a rotating glassy carbon disk electrode. The MoS_3-CV films displayed high catalytic activity for hydrogen evolution; the activity was higher in more acidic solutions. A typical film (made by 25 scanning cycles) on a glassy carbon disk gave current densities of 14 and 160 mA/cm^2 at overpotentials (η) of 200 and 300 mV, respectively, at pH

dx.doi.org/10.1021/ar5002022 | Acc. Chem. Res. 2014, 47, 2671−2681

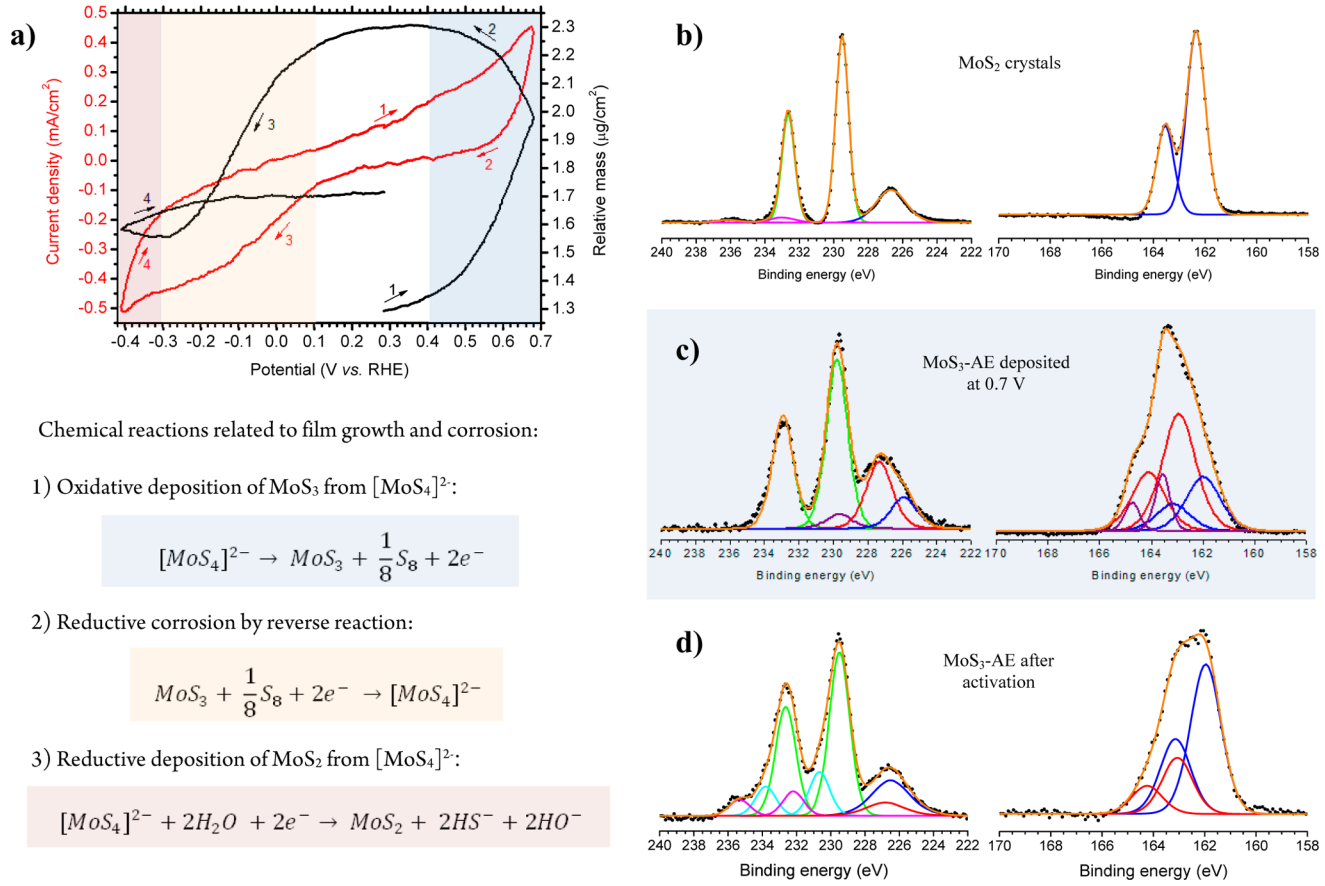

Chemical reactions related to film growth and corrosion:

1) Oxidative deposition of MoS_3 from $[MoS_4]^{2-}$:

$$[MoS_4]^{2-} \rightarrow MoS_3 + \frac{1}{8}S_8 + 2e^-$$

2) Reductive corrosion by reverse reaction:

$$MoS_3 + \frac{1}{8}S_8 + 2e^- \rightarrow [MoS_4]^{2-}$$

3) Reductive deposition of MoS_2 from $[MoS_4]^{2-}$:

$$[MoS_4]^{2-} + 2H_2O + 2e^- \rightarrow MoS_2 + 2HS^- + 2HO^-$$

Figure 2. (a) Top: Evolution of the current density (red line) and film mass (black line) during a potential scanning cycle for the electrochemical deposition of a molybdenum sulfide film. Arrows and numbers indicate the direction of potential scanning. Conditions: Au substrate, $NaClO_4$ electrolyte (0.1 M), 2 mM $(NH_4)_2[MoS_4]$, scan rate = 50 mV/s. Bottom: Chemical reactions related to film growth and corrosion. (b) XPS spectra of MoS_2 microcrystals. Left: Mo 3d and S 2s region; experimental data (····), fitting envelope (orange line), MoS_2 (green line), MoO_3 (magenta line), S^{2-} 2s (blue line). Right: S 2p region; experimental data (····), fitting envelope (orange line), MoS_2 (blue line). (c) XPS spectra of a MoS_3-AE film grown by potentiostatic anodic electrodeposition at 0.7 V vs RHE. Left: Mo 3d and S 2s region; experimental data (····), fitting envelope (orange line), MoS_3 (green line), S^0 2s (purple line), S_2^{2-} 2s (red line), S^{2-} 2s (blue line). Right: S 2p region; experimental data (····), fitting envelope (orange line), S^0 (purple line), S_2^{2-} (red line), S^{2-} (blue line). (d) XPS spectra for MoS_3-AE after activation for the HER. Left: Mo 3d region; experimental data (····), fitting envelope (orange line), Mo^AS_n (green line), $Mo^BO_aS_b$ (light-blue line), MoO_3 (magenta line), S_2^{2-} 2s (red line), S^{2-} 2s (blue line). Right: S 2p region; experimental data (····), fitting envelope (orange line), S_2^{2-} (red line), S^{2-} (blue line). Adapted from ref 21. Copyright 2013 American Chemical Society.

0.[18] The Tafel slope was 40 mV per decade, indicative of a rate-determining ion + atom step. Bulk electrolysis confirmed the quantitative Faradaic efficiency for the HER with this catalyst. The catalyst was active for hydrogen evolution over a wide range of pHs (e.g., 0 to 13).[18] The catalyst slowly deactivated in alkaline solutions but was stable in neutral and acidic solutions for many hours.[19]

At the time of our first report, the preparation of single-layer crystalline MoS_2 electrocatalysts required sophisticated and energy-intensive synthetic procedures, including ultrahigh-vacuum conditions, reduction by H_2S streams, and annealing at high temperatures.[9,20] Our electrodeposition method provided an easier and more scalable access to molybdenum sulfide-based HER catalysts.

Characterization of the electrodeposited molybdenum sulfide films then revealed the amorphous nature of the films. No diffraction patterns were observed in electron and X-ray diffraction analyses. X-ray photoelectron spectroscopy (XPS) analysis of the films indicated different compositions of the films depending on the potential region where the potential cycling experiment ended. For films grown by potential cycling experiments ending at an anodic potential, the XPS spectra resembled those of amorphous MoS_3 particles. These catalysts were tentatively labeled as MoS_3-CV. For films grown by cycling experiments ending at a cathodic potential, the XPS spectra resembled those of MoS_2. These catalysts were labeled as MoS_2-CV. The MoS_3-CV and MoS_2-CV films, however, exhibited similar HER activities, probably because they were activated to a similar catalyst during the HER. A study was then undertaken to understand the formation and activation of these catalysts.

GROWTH AND ACTIVATION OF AMORPHOUS MOLYBDENUM SULFIDE CATALYSTS

The first few cyclic voltammograms during the deposition of an amorphous molybdenum sulfide catalyst were featureless (Figure 1a). After several scans, a significant oxidative current was observed at the positive limit of the potential window (i.e., 0.5 to 0.7 V vs RHE) and a cathodic current was observed at the negative limit of the potential window (i.e., −0.3 to −0.4 V vs RHE). The growth of the catalyst was studied using an electrochemical quartz crystal microbalance (EQCM).[21]

dx.doi.org/10.1021/ar5002022 | Acc. Chem. Res. 2014, 47, 2671−2681

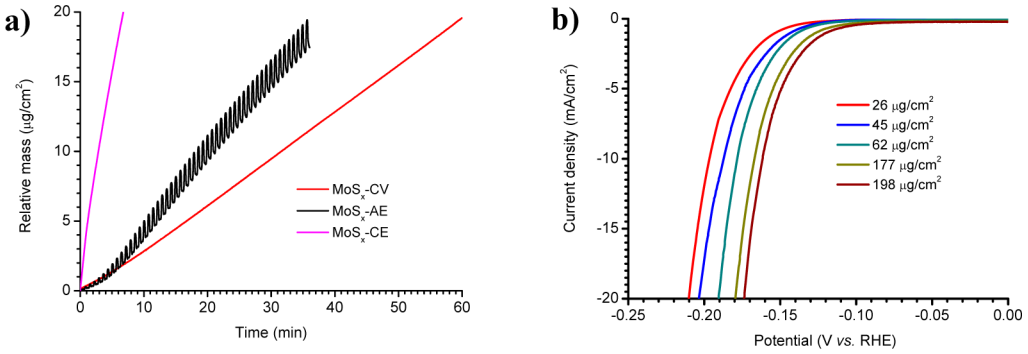

Figure 3. (a) Time-dependent growth of molybdenum sulfide films deposited by three different deposition methods: anodic electrolysis (AE) at 0.7 V, cathodic electrolysis (CE) at −0.4 V, and cyclic voltammetry (CV) between 0.7 and −0.4 V. (b) Stable (10th) polarization curves in 1.0 M H_2SO_4 for MoS_3 films with different loadings. Conditions: Au substrate; scan rate = 5 mV/s. Adapted from ref 21. Copyright 2013 American Chemical Society.

EQCM is a powerful tool for studying electron transfer processes coupled to small changes of mass on an electrode. Setting a high gain on the frequency-to-voltage converter of the EQCM enabled a detailed investigation of the mass changes during a single cycle of deposition. The deposition potential window was kept at 0.7 to −0.4 V vs RHE, while the starting point was chosen at 0.3 V since initial experiments showed no change in mass at this potential. Starting from 0.3 V, the potential was first polarized positively to 0.7 V, reversed from 0.7 to −0.4 V, and then reversed again to 0.3 V. The mass change during the sixth deposition cycle is represented in Figure 2a. The mass of the film increased in the potential region from 0.3 to 0.7 V, decreased in the region from 0.2 to −0.2 V, and increased again from −0.25 to −0.4 V. On the basis of previous studies of the electrochemistry of $[MoS_4]^{2-}$,[22,23] the oxidative deposition process was attributed to the oxidation of $[MoS_4]^{2-}$according to eq 1 in Figure 2a. This oxidation produced not only MoS_3 but also elemental S. The reductive corrosion from 0.2 to −0.3 V consumed 70% of the newly deposited mass. Reduction of MoS_3 to MoS_2 would not amount to this weight loss. The reaction was assigned to the reverse reaction of eq 1 (i.e., eq 2 in Figure 2a). Following this corrosion, a new reductive deposition took place between −0.25 and −0.4 V. This reaction was assigned to a reduction of $[MoS_4]^{2-}$ to form amorphous MoS_2, SH^-, and OH^- (eq 3 in Figure 2a). The repetitive deposition and corrosion sequence during an individual scanning cycle resulted in a staircase growth of the film, as shown by the black trace in Figure 3a.

EQCM was then applied to monitor the film growth under various deposition conditions.[21] It was found that a higher concentration of $[MoS_4]^{2-}$ in the deposition bath resulted in faster deposition. The potential window, especially the negative potential limit, also had an influence on the film growth. This influence was due to the potential-dependent corrosion of MoS_3 according to eq 2 at the cathodic potentials.

According to eqs 1−3, potential cycling would always produce a molybdenum sulfide film that is a mixture of amorphous MoS_3, MoS_2, and other sulfur species. On the other hand, electrolysis at a constant positive or negative potential would yield a "pure" amorphous MoS_3 or MoS_2 film. The EQCM was used to monitor the film growth at 0.7 V and at −0.4 V. Indeed, with constant-potential electrolysis, only constant film growth, but not corrosion, was observed (Figure 3a). Oxidative deposition at 0.7 V is the fastest method to grow a film, followed by potential cycling between 0.7 and −0.4 V. Reductive electrolysis at −0.4 V is the slowest method to deposit a film. The activities of the three films grown by oxidative electrolysis, potential cycling, and reductive electrolysis were compared. For films of the same mass (15 $\mu g/cm^2$), the activities were roughly the same. This was an indication that the three different films might be transformed to the same active species during catalysis.

Amorphous MoS_3 films grown by oxidative electrolysis were then used to benchmark the catalytic activity of this class of catalysts. Figure 3b shows the activities of films at different loadings. Within the range of 26 to 198 $\mu g/cm^2$, the activity increased with increasing loading while the Tafel slopes remained at about 40 mV/decade. At a loading of about 200 $\mu g/cm^2$, which is the conventional loading of Pt in fuel cells, the catalyst gave a current density of 10 mA/cm^2 at an overpotential of 160 mV (see Table 1 below for a comparison of the electrochemical HER performance parameters for the different amorphous catalysts presented in this Account).

As different deposition methods yielded molybdenum sulfide films of different compositions, these films were analyzed by XPS together with MoS_2 microcrystals.[21] For MoS_2 crystals, the Mo 3d spectrum is dominated by a doublet with a Mo $3d_{5/2}$ binding energy of 229.5 eV (Figure 2b). This doublet is attributed to the Mo^{IV} ion in MoS_2. A small doublet with a Mo $3d_{5/2}$ peak at 232.7 eV is also visible. This binding energy corresponds to that of Mo^{VI} ion, as in MoO_3. The S 2s peak at 226.7 eV is also visible in the Mo region. The S 2p spectrum shows one doublet with S $2p_{3/2}$ binding energy of 162.4 eV, corresponding to the sulfide (S^{2-}) ligand in MoS_2. The Mo:S ratio is 1:1.9; the Mo^{VI} ion contributes to 4% of the total Mo ions at the surface.

Potentiostatic anodic electrodeposition (AE) at 0.7 V vs RHE yielded amorphous MoS_3 plus some elemental sulfur according to eq 1. The XPS spectra of this film (Figure 2c) shows one Mo doublet with a $3d_{5/2}$ binding energy of 229.8 eV, corresponding to Mo^{IV} in MoS_3. Three different sulfur states were used to fit the S 2s and S 2p spectra.[21] The S $2p_{3/2}$ peaks have binding energies of 163.6, 162.9, and 162 eV, corresponding to elemental S^0, bridging S_2^{2-}, and terminal S^{2-}, respectively. The relative intensities of the peaks at 162.9 and 162.0 eV, however, could not be used to accurately deduce the S_2^{2-}/ S^{2-} ratio in the sample because of possible overlaps. The shapes and binding energies of the XPS spectra of the films are similar to those of previously reported amorphous MoS_3 particles and films.[16,22] The Mo:S ratio is 1:3.6, consistent with the presence of residual elemental sulfur as predicted by eq 1. The XPS spectra of films made by cathodic electrolysis and

dx.doi.org/10.1021/ar5002022 | Acc. Chem. Res. 2014, 47, 2671−2681

potential cycling methods also revealed compositions that were consistent with eqs 1−3.[21]

Activation of the MoS_3-AE film was followed using XPS and EQCM. Immersing the as-prepared film in 1.0 M H_2SO_4 seemed to remove most of the residual elemental sulfur, as indicated by a decrease in the Mo:S ratio to 1:3.2 and a mass loss of 7%.[21] The acid-washed MoS_3 film was then transformed to the active catalyst by a linear potential sweep. A mass decrease of 17% was observed at potentials just positive of the onset potential for the HER (Figure 4). This mass decrease is

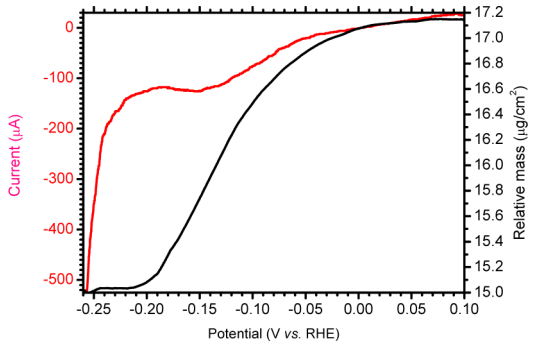

Figure 4. Mass change during the activation of a MoS_3 film in the first linear sweep scan. Conditions: Au substrate, H_2SO_4 electrolyte (1 M), scan rate = 5 mV/s. Adapted from ref 21. Copyright 2013 American Chemical Society.

consistent with the removal of slightly less than 1 equiv of S from MoS_3. Figure 2d shows the XPS spectra for the activated catalyst. The Mo 3d spectrum contains small peaks due to Mo^{IV} in molybdenum oxysulfide and Mo^{VI} in MoO_3 in addition to a dominating doublet due to Mo^{IV} in Mo sulfide. The S 2p spectrum shows two doublets due to S^{2-} and S_2^{2-}. The Mo:S ratio was close to 1:2, and the relative intensity of the S^{2-} and S_2^{2-} peaks was about 70 to 30. Importantly, the active species for amorphous molybdenum sulfide films made by cathodic electrolysis and potential cycling have the same XPS spectra. Therefore, all these films are transformed to the same active catalyst during the HER. This catalyst is labeled as MoS_{2+x} because it has a Mo/S ratio close to 2 but a S 2p XPS spectrum that is distinct from that of crystalline MoS_2 and indicates the presence of both S^{2-} and S_2^{2-} units.

The amorphous MoS_{2+x} catalyst should thus be distinguished from the ubiquitous MoS_2 nanocrystals by its different structure (amorphous vs crystalline) and XPS properties (vide supra). While metallic edge sites are the active sites for the HER catalyzed by MoS_2 nanoparticles, there are no defined edges in amorphous MoS_{2+x} films. However, chemically speaking, the edge sites in MoS_2 crystals can be considered as Mo and S sites that are coordinatively unsaturated. These unsaturated sites can adsorb hydrogen and mediate the HER. In the MoS_{2+x} films, there are plenty of such unsaturated "defect" Mo and S sites because of its amorphous nature. As a consequence, these amorphous films exhibit remarkablly high HER activities.

PROMOTION OF THE HER ACTIVITY OF AMORPHOUS MOLYBDENUM SULFIDE FILMS BY FIRST-ROW TRANSITION METAL IONS

Thin films active for the HER were also deposited from aqueous solution of $(NH_4)_2[Co(MoS_4)_2]$ by cyclic voltammetry. The optimized deposition conditions were analogous to those for the deposition of amorphous molybdenum sulfide films. Similar films could be made from solutions containing a mixture of $CoCl_2$ and $(NH_4)_2[MoS_4]$. Presumably, $(NH_4)_2[Co(MoS_4)_2]$ formed in this mixture was the precursor

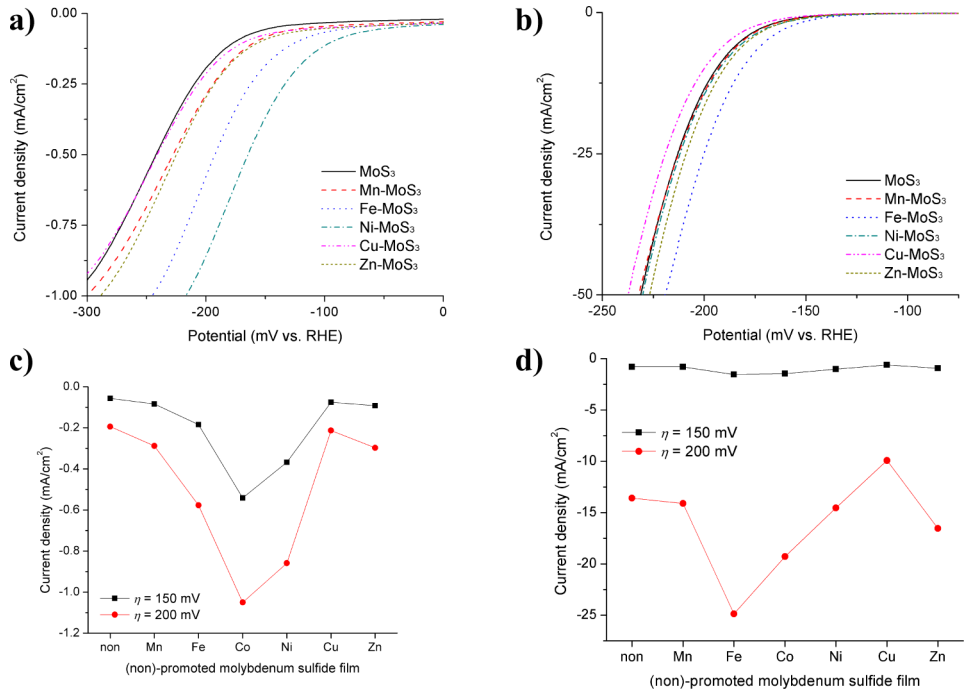

Figure 5. (a, b) Polarization curves of unpromoted and M-promoted (M = Mn, Fe, Ni, Cu, Zn) MoS_{2+x} films on glassy carbon at (a) pH 7 and (b) pH 0. The M-promoted films were deposited from aqueous solutions of M^{2+} (0.67 mM) and $[MoS_4]^{2-}$ (2 mM) by 25 consecutive cyclic voltammetric scans. (c, d) Comparison of current densities of unpromoted and M-promoted MoS_{2+x} films on glassy carbon at (c) pH 7 and (d) pH 0 at η = 150 and 200 mV. Adapted with permission from ref 24. Copyright 2012 Royal Society of Chemistry.

dx.doi.org/10.1021/ar5002022 | Acc. Chem. Res. 2014, 47, 2671−2681

for the films. Deposition from solutions of $CoCl_2$ and $(NH_4)_2[MoS_4]$ allowed the Co:Mo ratio in the deposition bath to be varied. XPS analysis of the films revealed the presence of Mo, Co, and S. The Co−Mo−S films are active for the HER; in fact, their activity is higher than that of the MoS_{2+x} catalyst.[24] The addition of cobalt and nickel to MoS_2 nanoparticles is known to enhance their catalytic activity for the hydrodesulfurization reaction.[25] Bonde et al.[20] also showed that Co^{2+} promotes the activity of MoS_2 and WS_2 nanocrystals for the HER. This prompted us to investigate the promotion of the HER activity of MoS_{2+x} by Co and several other first-row transition metal ions. The ions were in the +2 oxidation state.

Figure 5 shows the catalytic activity of the ternary M−MoS_{2+x} films (M = Mn, Fe, Co, Ni, Cu, Zn) at pH 7 and 0.[26] Fe, Co, and Ni ions are effective promoters, while Mn, Cu, and Zn ions give no or only a small promotion. At pH 7, the best promoter is Co^{2+}, which gives MoS_{2+x} a 5-fold increase in current density at η = 200 mV. At pH 0, the best promoter is Fe^{2+}, which gives MoS_{2+x} a 2-fold increase in current density at both η = 200 mV and η = 150 mV. In general, the promotion by the same ion is stronger at pH 7 than at pH 0.

The origin of the promotional effects of Fe, Co, and Ni ions was probed. The morphology and thickness of the MoS_{2+x} and M-MoS_{2+x} films were studied by scanning electron microscopy (SEM). Incorporation of Fe, Co, or Ni ions resulted in an appreciable increase in the porosity of the film. The thickness of the film also increased considerably after the incorporation of Fe, Co, or Ni ions. The unpromoted MoS_{2+x} film had a maximum thickness of 150 nm, while the Fe, Co, and Ni-promoted films had thicknesses of up to 500 nm under the same deposition conditions. The compositions of the films were determined by XPS and inductively coupled plasma atomic emission spectroscopy (ICP-AES). It was found that only a low amount of Mn, Cu, or Zn ions (1−5%) could be incorporated to the MoS_{2+x} films, which was the reason for their lack of promotion of the activity of these films. On the other hand, significant amounts of Fe, Co, and Ni ions could be incorporated. From a deposition bath containing a 1:3 ratio of MCl_2 (M = Fe, Co, Ni) to $(NH_4)_2[MoS_4]$, M-MoS_{2+x} films with a M:Mo ratio between 1:3 and 1:4 could be deposited. In addition, the M-MoS_{2+x} films (M = Fe, Co, Ni) had a Mo content that was about 3 times that of the unpromoted MoS_{2+x} film grown under analogous conditions. This indicates that Fe, Co, and Ni ions promoted the growth of the MoS_{2+x} films. The relative electrochemical surface areas of the unpromoted and Fe, Co, and Ni-promoted MoS_{2+x} films were compared using their double-layer capacitances, which could be determined by cyclic voltammetry. The Fe, Co, and Ni-promoted MoS_{2+x} films had surface areas that were 1.4−3.3 times of that of the unpromoted MoS_{2+x} film.

The above data indicate that Fe, Co, and Ni ions promote the growth of the MoS_{2+x} film, increasing its thickness, loading, porosity, and surface area. This increase is on the order of 3-fold. At pH 0, the increase in activity by promotion is on the order of 3-fold as well. Therefore, the promotion at pH 0 is mostly associated with film growth. At pH 7, however, the promoted films are 5−12 times more active. Clearly, at higher pHs the Fe, Co, and Ni ions seem to increase the intrinsic activity of MoS_{2+x} for the HER. It is hypothesized that these ions modify the absorption energy of hydrogen at the unsaturated Mo and S sites that are the active sites for the HER. Similar promotional effects are known for the hydrodesulfurization reaction of natural gas and refined petroleum products and the HER, where transition-metal ions such as Co^{2+} significantly enhance the activity of MoS_2 nanoparticles.[12,20,25,27] DFT calculations have suggested that Co ions bind to inactive sulfur edge sites, making them catalytically active.[20]

CHEMICALLY SYNTHESIZED AMORPHOUS MOLYBDENUM SULFIDE PARTICLES

While highly active amorphous molybdenum sulfide films could be prepared by electrodeposition as described in the previous sections, the preparation of similarly active nanoparticles through chemical synthesis is also desirable. Chemical synthesis tends to be more scalable and can allow the deposition of catalyst films without the use of electrochemistry, which might be unsuitable for certain substrates. As our earlier work showed that an amorphous MoS_3 film could be activated to form the active MoS_{2+x} catalyst, we thought amorphous MoS_3 particles might have the same property. Amorphous MoS_3 particles are normally prepared by acidification of tetrathiomolybdate solutions.[28] We found that similar particles could be obtained by acidification of a solution of MoO_3 and Na_2S, making the synthesis more economical.[29] The XPS spectra of the resulting MoS_3 particles resemble those of known MoS_3 samples.[16] The Mo:S ratio is 1:3. Figure 6a shows a TEM image of the particles. An electron diffraction study confirmed the amorphous nature of the particles.

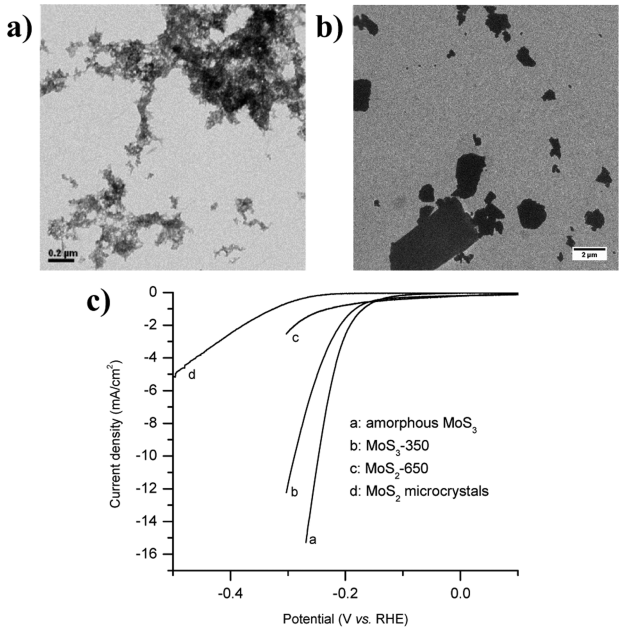

Figure 6. (a, b) TEM images of amorphous MoS_3 particles (a) before and (b) after annealing at 350 °C for 1 h. (c) Polarization curves for carbon-paste electrodes modified with a layer of MoS_x species. The measurements were conducted at pH 0 (1.0 M H_2SO_4) at a scan rate of 5 mV/s. Adapted with permission from ref 29. Copyright 2012 Royal Society of Chemistry.

The chemically synthesized amorphous MoS_3 particles were deposited on various electrodes by drop-casting and spray-casting methods. The resulting electrodes had rather good activity for the HER at pH 0. For example, at a loading of 32 $\mu g/cm^2$, a MoS_3-modified glassy carbon electrode gave a current density of 2.3 mA/cm^2 at η = 200 mV. This activity is comparable to those of many nanostructured and crystalline

dx.doi.org/10.1021/ar5002022 | Acc. Chem. Res. 2014, 47, 2671−2681

MoS_2 particles, although it is only one-eighth of that of an amorphous MoS_{2+x} film at a similar loading.[21] Importantly, the amorphous MoS_3 particles also underwent an activation process to form an active species that has XPS spectra similar to those of the MoS_{2+x} species formed from amorphous MoS_3 films. This indicates that the active species from chemically synthesized MoS_3 particles is also MoS_{2+x}.

Annealing of amorphous MoS_3 particles resulted in a significant change in composition and crystallinity. After the particles were annealed at 350 °C for 1 h, the particle size increased from below 100 nm to about 1 μm (compare panels a and b in Figure 6), and the particles became polycrystalline. The composition remained close to MoS_3. When further annealed at 650 °C for 30 min, the particles became single-crystalline MoS_2 particles that were 100 nm in width and several micrometers in length. Even larger microcrystals of MoS_2 could be purchased from Aldrich. The activities of various molybdenum sulfide particles were compared using identical carbon-paste electrodes as the substrates (Figure 6c). The amorphous MoS_3 particles had the highest activity, followed by polycrystalline MoS_3 (annealed at 350 °C, labeled as MoS_3-350) and then the small MoS_2 single-crystal particles (annealed at 650 °C, labeled as MoS_2-650). The larger MoS_2 microcrystals had the lowest activity. The activity trend is consistent with our hypothesis for the high activity of amorphous molybdenum sulfide catalysts. In the amorphous MoS_3 particles, there are a large number of unsaturated Mo and S sites that might catalyze the HER. When annealed at high temperatures, the particles become more crystalline, so there are fewer such "defect" sites. Finally, the largest crystals have the least amount of defect sites.

The Tafel slopes of chemically synthesized amorphous MoS_3 particles were larger than those of electrochemically deposited MoS_{2+x} films. The latter were constantly about 40 mV/decade, while the former were as high as 63 mV/decade. Moreover, a higher loading of MoS_3 particles led to a higher Tafel slope. This is illustrated in Figure 7a. At a loading of 28 μg/cm^2, a glassy carbon electrode modified with MoS_3 particles gave a Tafel slope of 47 mV/decade; at a loading of 282 μg/cm^2, an analogous electrode gave a Tafel slope of 63 mV/decade. We thought that the higher Tafel slopes observed for MoS_3 particles, especially at higher loadings, might be due to slow electron transport in this type of material, which has modest electronic conductivity. This was confirmed by electrochemical impedance spectroscopy.[30] The equivalent circuit that fits the impedance data is shown in Figure 7b. This is a transmission line model that was previously used to model porous materials with intermediate resistivity (e.g., TiO_2 films in Grätzel cells).[31] The porous and resistive nature of MoS_3 particles is taken into account by repeating units of R_m in series with R_{ct}, where R_m represents a non-negligible electronic resistance of MoS_3 and R_{ct} represents the charge transfer resistance due to the HER. Figure 7c shows the fitting of the Nyquist plot for the HER by MoS_3 particles at a loading of 282 μg/cm^2. A notable feature is the 45° line observed in the high-frequency region, which originates from the slow electron transport process. Consequently, this feature was designated as a fingerprint for slow electron transport in an electrocatalytic process. The fit of the impedance data also yielded a charge transfer resistance R_{ct} that is inversely proportional to the HER rate. The linear fit of the plot of log R_{ct} versus overpotential gives the charge-transfer Tafel slope. It was found that the slopes were about 40 mV/decade for MoS_3 particles at both low and high loadings. Thus,

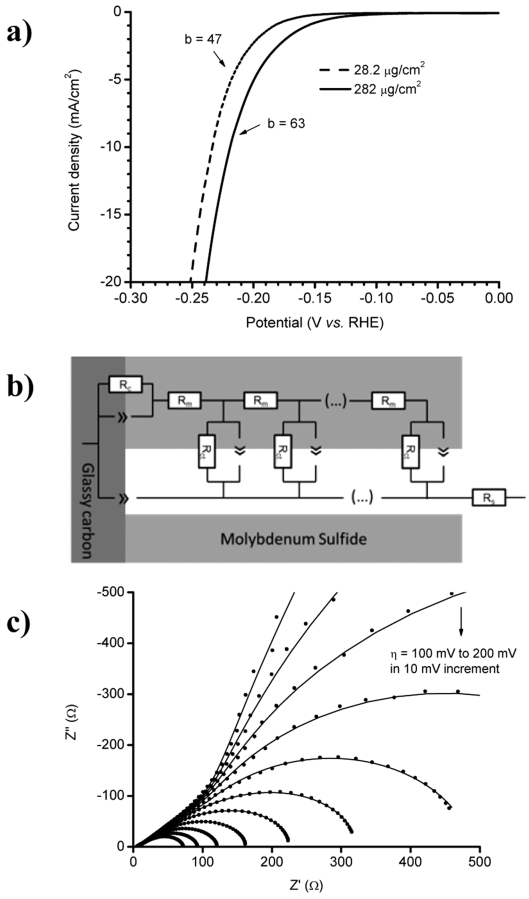

Figure 7. (a) Polarization curves for glassy carbon electrodes modified with two different loadings of amorphous MoS_3 particles at pH 0. (b) Equivalent circuit using a transmission line model. R_c represents the resistance at the contact between the electrode and the catalyst film. R_m is the non-negligible electronic resistance of MoS_x. R_{ct} is the charge transfer resistance. The layer structure of the film is taken into account by repeating units of R_m in series with R_{ct}. (c) Nyquist plot and fits of the impedance response of the MoS_3-modified electrode at a loading of 282 μg/cm^2. Adapted with permission from ref 30. Copyright 2013 Royal Society of Chemistry.

the higher apparent Tafel slopes obtained from the voltammetric data reflect not only the electrode kinetics but also the slow electron transport process in the catalyst. Adding carbon black particles (Vulcan) to amorphous MoS_3 particles improved the conductivity of the system, resulting in a lower Tafel slope and an absence of the 45° line in the Nyquist impedance plot. Alternatively, more conductive amorphous molybdenum sulfide particles could be prepared by chemical reduction of $[MoS_4]^{2-}$ with $NaBH_4$. The resulting particles had XPS spectra similar to those of MoS_{2+x} and an apparent Tafel slope of less than 40 mV/decade at both low and high loadings (see Table 1).

PHOTOELECTROCHEMICAL HYDROGEN EVOLUTION FROM COPPER(I) OXIDE COATED WITH AN AMORPHOUS MOLYBDENUM SULFIDE CATALYST

The amorphous molybdenum sulfide catalysts, especially the electrodeposited films, exhibit many features that are attractive for photoelectrochemical hydrogen evolution: they can be deposited under ambient conditions using readily available and

dx.doi.org/10.1021/ar5002022 | Acc. Chem. Res. 2014, 47, 2671−2681

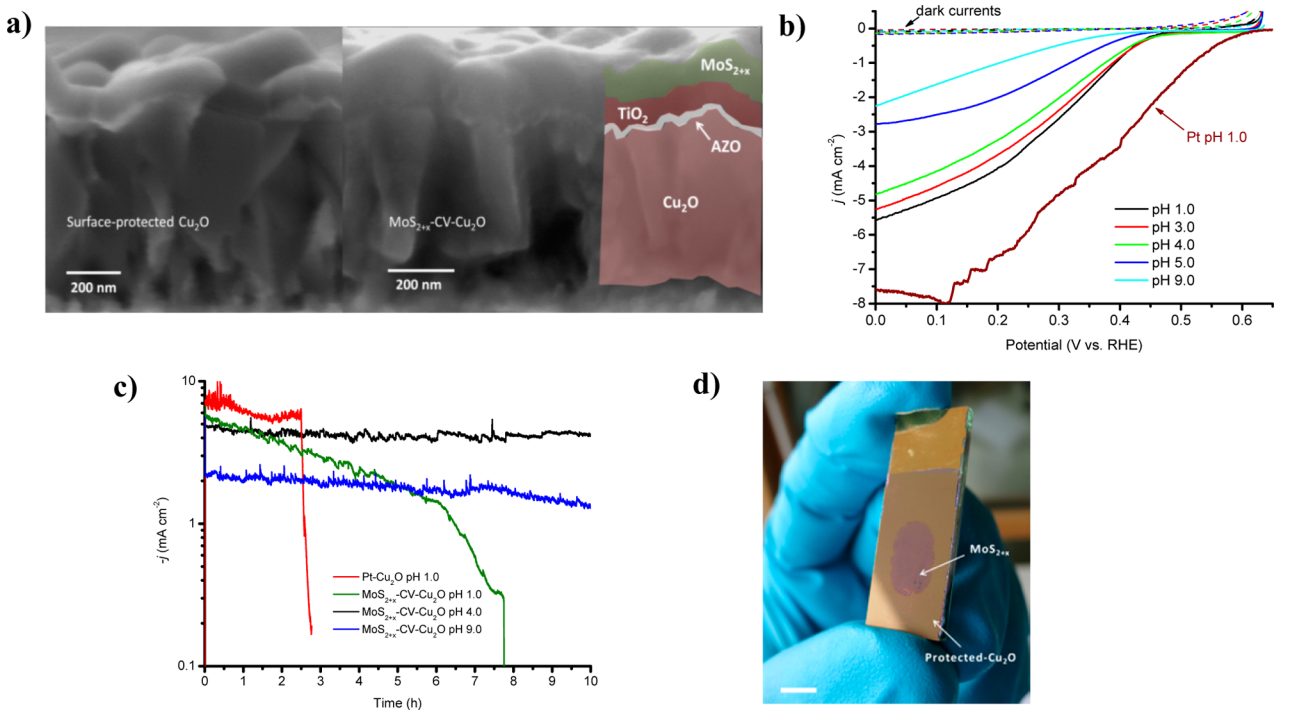

Figure 8. (a) Cross-sectional SEM images of (left) the protective layers (20 nm AZO and 100 nm TiO_2) on Cu_2O and (right) a ca. 100 nm thick MoS_{2+x} film on top of the protected Cu_2O electrode. (b) Current−potential curves under simulated AM 1.5 illumination (100 mW/cm^2) at different pH values for a MoS_{2+x}−Cu_2O photocathode (10th scan). Catalyst loading = 30 μg/cm^2. (c) Photocathode stability at 0 V vs RHE for Cu_2O photocathodes modified with different HER catalysts under AM 1.5 illumination. (d) Digital image of a MoS_{2+x}−Cu_2O photocathode. The scale bar corresponds to 5 mm. The area covered with the MoS_{2+x} catalyst (66 μg/cm^2) is in the middle of the photoelectrode and corresponds here to 0.48 cm^2. Adapted with permission from ref 32. Copyright 2014 Nature Publishing Group.

inexpensive precursors, they have high HER activity and stability, and they are optically rather transparent. Therefore, we collaborated with the Grätzel group at our institute to apply the MoS_{2+x} catalyst to promote the photoelectrochemical hydrogen evolution on Cu_2O.[32] Surface-protected cuprous oxide is arguably the state-of-the-art p-type oxide for photoelectrochemical hydrogen evolution.[33] It has a direct band gap of 2 eV and can produce a maximum photocurrent of 14.7 mA/cm^2 and exhibits a maximum solar to hydrogen efficiency of 18% under 1 sun irradiation. Pt[34] and RuO_2[35] had been used as the HER catalysts for Cu_2O in earlier studies.

The deposition of the molybdenum sulfide catalyst was achieved by photoelectrochemistry utilizing unfiltered irradiation from a Xe lamp. Under illumination, photons with energy greater than the band gap of Cu_2O are absorbed, generating electron−hole pairs in the metal oxide photoelectrode. Engineering of a p−n junction between the p-type cuprous oxide and a thin layer of n-type Al-doped ZnO (AZO) reduces electron−hole recombination and facilitates the extraction of electrons from the photoelectrode. Excited electrons are driven through the TiO_2 protective layer and into the semiconductor−electrolyte interface. Excited electrons reaching the electrolyte solution have enough chemical potential to drive the reductive deposition of MoS_2 (eq 3 in Figure 2a). The unfiltered irradiation has a small fraction of photons with enough energy to create holes in the TiO_2 that under the applied bias drive the oxidative deposition of MoS_3 (eq 1 in Figure 2a). Overall, the photoelectrochemical deposition of the MoS_{2+x} catalyst is analogous to the electrochemical deposition of the same catalyst in the dark. Figure 8a shows the surface-protected Cu_2O before and after the deposition of a 100 nm thick layer of catalyst.

The MoS_{2+x}−Cu_2O photocathodes were tested for hydrogen evolution under simulated AM 1.5 illumination (100 mW/cm^2). Figure 8b displays the current density−potential curves in the dark and under illumination for a MoS_{2+x}−Cu_2O photocathode with a catalyst loading of 30 μg/cm^2. A photocurrent density of −5.7 mA/cm^2 at 0 V vs RHE was obtained at pH 1. The onset potential is 150 mV more negative than that observed for an analogous photocathode with Pt nanoparticles as the HER catalyst. However, the deposition of the conformal film protects the photocathode from corrosion in acid, improving the stability of the photoelectrode relative to an analogous device coated with Pt nanoparticles (Figure 8c). The MoS_{2+x}−Cu_2O photoelectrode is also stable and active at neutral and basic pH. Stable current densities of −4 and −2 mA/cm^2 were obtained at 0 V vs RHE at pH 4 and 9, respectively, for 10 h. The photoelectrochemical hydrogen evolution has a nearly quantitative Faradaic efficiency.

The catalyst loading can be varied from 10 to 100 μg/cm^2, and the catalyst can be deposited on surface areas on the order of several square centimeters. Figure 8d shows a digital image of the surface-protected Cu_2O electrode after deposition of the MoS_{2+x} catalyst on the area exposed to light. This layered device is the most active and stable Cu_2O photoelectrode that makes use of an earth-abundant HER catalyst.

dx.doi.org/10.1021/ar5002022 | Acc. Chem. Res. 2014, 47, 2671−2681

Table 1. Summary of Electrochemical HER Parameters of the Amorphous Molybdenum Sulfide Catalysts Developed in Our Group

catalyst	preparation method (substrate)	catalyst loading (mg/cm^2)	$\eta_{j=10\ mA/cm^2}$ at pH 0 (mV)	Tafel slope at pH 0 (mV/decade)
MoS_{2+x} film[a]	electrochemical (GC and Au)	0.2	160	40
M-MoS_{2+x} films[b]	electrochemical (GC)	0.013−0.014[e]	181−192	39−43
MoS_3 particles[c]	chemical synthesis (GC)	0.282	220	63
		0.028	235	45
MoS_{2+x} particles[d]	chemical reduction (Vulcan)	0.252	200	35
		0.025	225	36

[a]Deposited by cyclic voltammetry from a $[MoS_4]^{2-}$ precursor solution.[21] [b]Deposition from a bath containing a 1:3 ratio of MCl_2 to $(NH_4)_2[MoS_4]$ by cyclic voltammetry, where M = Fe, Co, or Ni.[24] [c]Chemical synthesis through acidification of a solution of MoO_3 and Na_2S.[29,30] [d]Chemical reduction of $[MoS_4]^{2-}$ with $NaBH_4$.[30] [e]Loading of Mo.

RELATED SYNTHESES AND APPLICATIONS OF AMORPHOUS MOLYBDENUM SULFIDE CATALYSTS

Since our initial report in 2011, several other groups have worked on the development of analogous amorphous molybdenum sulfide catalysts. Benck et al.[36] reported the synthesis of amorphous molybdenum sulfide particles from a solution of ammonium heptamolybdate, sodium sulfide, and sulfuric acid. The resulting catalyst has properties and activity similar to our chemically prepared MoS_3 precatalyst. Laursen et al.[37] electrochemically deposited amorphous MoS_{2+x} films on activated carbon paper to achieve higher mechanical stability of the catalyst. Hsu et al.[38] prepared amorphous molybdenum sulfide particles by low-temperature thermolysis of an ammonium tetrathiomolybdate precursor. The addition of $NbCl_5$ during the preparation of the catalyst resulted in enhancement of the HER activity. The same group also deposited amorphous molybdenum sulfide catalysts on high-surface-area three-dimensional electrodes for electrochemical hydrogen production using this thermolysis method.[39,40]

A number of highly active amorphous HER catalysts have recently been developed using electrochemical deposition methods similar to the one developed for the deposition of amorphous molybdenum sulfide film catalysts.[41−43] Tran et al.[42] reported the electrodeposition of ternary sulfides of cobalt−tungsten and nickel−tungsten that showed good HER activity. Wang et al.[43] reported a simple one-step electrochemical copolymerization method to fabricate a hybrid film containing polypyrrole (PPy), a conductive polymer, and an amorphous molybdenum sulfide catalyst. The hybrid system exhibited a remarkable HER activity. Sun et al.[41] reported the electrochemical synthesis of an amorphous Co−S catalyst that worked best in neutral water.

Our amorphous MoS_{2+x} catalysts have also been adapted by other groups for photoelectrochemical hydrogen evolution. Seger et al.[44] deposited the MoS_{2+x} film catalyst on a Si photoelectrode protected with a Ti layer. The resulting photocathode gave an impressive photocurrent under illumination. The same group also deposited this catalyst on Si photocathodes protected by a thin MoS_2 layer.[45] Tran et al.[46] reported similar work using the MoS_{2+x} film catalyst for photoelectrochemical hydrogen evolution on silicon nanowires. Bourgeteau et al.[47] applied amorphous MoS_3 particles as a HER catalyst to an organic solar cell for photoelectrochemical hydrogen evolution in acidic solutions. In related work, Tang et al.[48] deposited an amorphous molybdenum sulfide catalyst on CdSe-seeded CdS nanorods by microwave thermolysis of $(NH_4)_2MoS_4$. Characterization of the catalyst by XPS and extended X-ray absorption fine structure (EXAFS) spectroscopy revealed an active catalyst similar to our MoS_{2+x} species. The catalyst promoted the photochemical hydrogen production from a buffered aqueous solution (pH 7) using triethanolamine as the sacrificial electron donor.

CONCLUSION AND PERPECTIVES

To sum up, we have established amorphous molybdenum sulfides as a new class of nonprecious HER catalysts. These catalysts can be conveniently synthesized either by electrodeposition or by a wet-chemical process. The mechanism for the electrodeposition has been unveiled, and the active species has been identified as MoS_{2+x}. The catalysts exhibit remarkable HER activities, especially in acidic solutions, rivaling those of the best-known catalysts that are composed of only earth-abundant elements. Table 1 summarizes important performance parameters (apparent Tafel slope, catalyst loading, and overpotential necessary to produce a current density of 10 mA/cm^2) for the amorphous molybdenum sulfide systems developed in our group and described in this Account.

Parallel to our work, a large amount of research effort has been invested in the development of nanostructured and single-crystalline MoS_2 nanoparticles.[12] While our amorphous catalysts have activities similar to those of the best MoS_2 nanocrystals, they can be prepared under ambient conditions using solution-based methods. The MoS_2 nanocrystals, on the other hand, are normally prepared under elevated temperature, pressure, or vacuum. Clearly, the amorphous molybdenum sulfide catalysts are more processable and scalable. This aspect has been demonstrated in several applications of the amorphous catalysts in photoelectrochemical hydrogen evolution, including our own work on MoS_{2+x}-coated Cu_2O photocathodes.

The production of solar fuels is a grand technical challenge that has inspired numerous scientific endeavors. Not all work will lead to the ultimate solution, if such a solution exists. Likewise, not all promising catalysts (including the amorphous molybdenum sulfide catalysts described here) may end up being used in an actual energy conversion device. The broader implication of our research in this field, however, is the concept of using amorphous materials as catalysts for hydrogen evolution. Amorphous materials are often accessible through simple solution-based syntheses under relatively mild conditions. The structural disorder in these materials might be detrimental to their electronic and photonic properties, but for catalytic applications, the resulting defect sites may serve as efficient reaction centers. We expect the emergence of amorphous catalysts for solar fuel production in the near future. The difficulty in the characterization and understanding

dx.doi.org/10.1021/ar5002022 | Acc. Chem. Res. 2014, 47, 2671−2681

of such catalysts will motivate the development of new analytical tools in catalysis.

AUTHOR INFORMATION

Corresponding Author

*E-mail: xile.hu@epfl.ch. Tel.: +41 21 693 9781.

Notes

The authors declare no competing financial interest.

Biographies

Carlos G. Morales-Guio was born in Nobsa, Colombia. He obtained a Bachelor's degree in Chemical Engineering from Osaka University in 2011, where he was a Monbukagakusho Scholar. He then obtained a Master's degree in Chemical Engineering and Biotechnology at the École Polytechnique Fédérale de Lausanne (EPFL) in 2013. Currently, he is a Ph.D. student in Prof. Xile Hu's group at EPFL. His research focuses on the coupling of earth-abundant electrocatalysts to photoelectrodes for efficient solar fuel production.

Xile Hu was born in 1978 in Putian, China. He received a B.S. degree from Peking University in 2000 and a Ph.D. degree from the University of California, San Diego in 2004 (advisor: Prof. Karsten Meyer). He carried out a postdoctoral study at the California Institute of Technology (advisor: Prof. Jonas Peters) before joining the École Polytechnique Fédérale de Lausanne as a tenure-track assistant professor in 2007. He is currently an associate professor at the same institute. His research interests range from organometallic chemistry, synthetic methodology, and reaction mechanisms to biomimetic and biospeculated coordination chemistry to electrocatalysis and artificial photosynthesis.

ACKNOWLEDGMENTS

This work is dedicated to Professor Michael Grätzel on the occasion of his 70th birthday. This work was supported by a starting grant from the European Research Council under the European Community's Seventh Framework Programme (FP7 2007-2013)/ERC Grant Agreement 257096. We thank our co-workers, especially Dr. Daniel Merki and Dr. Heron Vrubel, for their contributions to this project.

REFERENCES

(1) Grätzel, M. Photoelectrochemical cells. *Nature* **2001**, *414*, 338–344.

(2) Lewis, N. S.; Nocera, D. G. Powering the planet: Chemical challenges in solar energy utilization. *Proc. Natl. Acad. Sci. U.S.A.* **2006**, *103*, 15729–15735.

(3) Momirlan, M.; Veziroglu, T. N. The properties of hydrogen as fuel tomorrow in sustainable energy system for a cleaner planet. *Int. J. Hydrogen Energy* **2005**, *30*, 795–802.

(4) Joshi, A. S.; Dincer, I.; Reddy, B. V. Exergetic assessment of solar hydrogen production methods. *Int. J. Hydrogen Energy* **2010**, *35*, 4901–4908.

(5) Pinaud, B. A.; Benck, J. D.; Seitz, L. C.; Forman, A. J.; Chen, Z. B.; Deutsch, T. G.; James, B. D.; Baum, K. N.; Baum, G. N.; Ardo, S.; Wang, H. L.; Miller, E.; Jaramillo, T. F. Technical and economic feasibility of centralized facilities for solar hydrogen production via photocatalysis and photoelectrochemistry. *Energy Environ. Sci.* **2013**, *6*, 1983–2002.

(6) *Photoelectrochemical Hydrogen Production*; van de Krol, R., Grätzel, M., Eds.; Electronic Materials: Science and Technology, Vol. *102*; Springer: New York, 2012.

(7) Hinnemann, B.; Moses, P. G.; Bonde, J.; Jørgensen, K. P.; Nielsen, J. H.; Horch, S.; Chorkendorff, I.; Nørskov, J. K. Biomimetic hydrogen evolution: MoS_2 nanoparticles as catalyst for hydrogen evolution. *J. Am. Chem. Soc.* **2005**, *127*, 5308–5309.

(8) Nørskov, J. K.; Bligaard, T.; Logadottir, A.; Kitchin, J. R.; Chen, J. G.; Pandelov, S.; Stimming, U. Trends in the exchange current for hydrogen evolution. *J. Electrochem. Soc.* **2005**, *152*, J23–J26.

(9) Jaramillo, T. F.; Jørgensen, K. P.; Bonde, J.; Nielsen, J. H.; Horch, S.; Chorkendorff, I. Identification of active edge sites for electrochemical H_2 evolution from MoS_2 nanocatalysts. *Science* **2007**, *317*, 100–102.

(10) Li, Y.; Wang, H.; Xie, L.; Liang, Y.; Hong, G.; Dai, H. MoS_2 nanoparticles grown on graphene: An advanced catalyst for the hydrogen evolution reaction. *J. Am. Chem. Soc.* **2011**, *133*, 7296–7299.

(11) Wang, H.; Lu, Z.; Xu, S.; Kong, D.; Cha, J. J.; Zheng, G.; Hsu, P.-C.; Yan, K.; Bradshaw, D.; Prinz, F. B.; Cui, Y. Electrochemical tuning of vertically aligned MoS_2 nanofilms and its application in improving hydrogen evolution reaction. *Proc. Natl. Acad. Sci. U.S.A.* **2013**, *110*, 19701–19706.

(12) Morales-Guio, C. G.; Stern, L.-A.; Hu, X. Nanostructured hydrotreating catalysts for electrochemical hydrogen evolution. *Chem. Soc. Rev.* **2014**, DOI: 10.1039/C3CS60468C.

(13) Laursen, A. B.; Kegnaes, S.; Dahl, S.; Chorkendorff, I. Molybdenum sulfides—Efficient and viable materials for electro- and photoelectrocatalytic hydrogen evolution. *Energy Environ. Sci.* **2012**, *5*, 5577–5591.

(14) Merki, D.; Hu, X. Recent developments of molybdenum and tungsten sulfides as hydrogen evolution catalysts. *Energy Environ. Sci.* **2011**, *4*, 3878–3888.

(15) Yan, Y.; Xia, B.; Xu, Z.; Wang, X. Recent development of molybdenum sulfides as advanced electrocatalysts for hydrogen evolution reaction. *ACS Catal.* **2014**, *4*, 1693–1705.

(16) Weber, T.; Muijsers, J. C.; Niemantsverdriet, J. W. Structure of amorphous MoS_3. *J. Phys. Chem.* **1995**, *99*, 9194–9200.

(17) Hibble, S. J.; Rice, D. A.; Pickup, D. M.; Beer, M. P. Mo K-edge EXAFS and S K-edge absorption studies of the amorphous molybdenum sulfides $MoS_{4.7}$, MoS_3, and $MoS_3{\cdot}nH_2O$ ($n \sim 2$). *Inorg. Chem.* **1995**, *34*, 5109–5113.

(18) Merki, D.; Fierro, S.; Vrubel, H.; Hu, X. L. Amorphous molybdenum sulfide films as catalysts for electrochemical hydrogen production in water. *Chem. Sci.* **2011**, *2*, 1262–1267.

(19) Merki, D. A. Ph.D. Thesis, Ecole Polytechnique Fédérale de Lausanne, Lausanne, Switzerland, 2012.

(20) Bonde, J.; Moses, P. G.; Jaramillo, T. F.; Nørskov, J. K.; Chorkendorff, I. Hydrogen evolution on nano-particulate transition metal sulfides. *Faraday Discuss.* **2009**, *140*, 219–231.

(21) Vrubel, H.; Hu, X. Growth and activation of an amorphous molybdenum sulfide hydrogen evolving catalyst. *ACS Catal.* **2013**, *3*, 2002–2011.

(22) Belanger, D.; Laperriere, G.; Girard, F.; Guay, D.; Tourillon, G. Physicochemical characteristics of electrochemically deposited molybdenum sulfide and polypyrrole tetrathiomolybdate molybdenum trisulfide composite electrodes. *Chem. Mater.* **1993**, *5*, 861–868.

(23) Ponomarev, E. A.; Neumann-Spallart, M.; Hodes, G.; Lévy-Clément, C. Electrochemical deposition of MoS_2 thin films by reduction of tetrathiomolybdate. *Thin Solid Films* **1996**, *280*, 86–89.

(24) Merki, D.; Vrubel, H.; Rovelli, L.; Fierro, S.; Hu, X. Fe, Co, and Ni ions promote the catalytic activity of amorphous molybdenum sulfide films for hydrogen evolution. *Chem. Sci.* **2012**, *3*, 2515–2525.

(25) Topsøe, H.; Clausen, B.; Massoth, F. In *Catalysis: Science and Techology*; Anderson, J., Boudart, M., Eds.; Springer: Berlin, 1996; Vol. *11*; pp 1–269.

(26) Here the films are labeled M-MoS_{2+x}, rather than M-MoS_3 as in the original paper. This was done because the active catalyst in various amorphous molybdenum sulfide catalysts is now known to be MoS_{2+x}. In the original paper, the MoS_3 label referred to the precatalyst.

(27) Besenbacher, F.; Brorson, M.; Clausen, B. S.; Helveg, S.; Hinnemann, B.; Kibsgaard, J.; Lauritsen, J. V.; Moses, P. G.; Nørskov, J. K.; Topsøe, H. Recent STM, DFT and HAADF-STEM studies of sulfide-based hydrotreating catalysts: Insight into mechanistic, structural and particle size effects. *Catal. Today* **2008**, *130*, 86–96.

(28) Afanasiev, P. Synthetic approaches to the molybdenum sulfide materials. *C. R. Chim.* **2008**, *11*, 159−182.
(29) Vrubel, H.; Merki, D.; Hu, X. Hydrogen evolution catalyzed by MoS_3 and MoS_2 particles. *Energy Environ. Sci.* **2012**, *5*, 6136−6144.
(30) Vrubel, H.; Moehl, T.; Grätzel, M.; Hu, X. Revealing and accelerating slow electron transport in amorphous molybdenum sulphide particles for hydrogen evolution reaction. *Chem. Commun.* **2013**, *49*, 8985−8987.
(31) Fabregat-Santiago, F.; Bisquert, J.; Garcia-Belmonte, G.; Boschloo, G.; Hagfeldt, A. Influence of electrolyte in transport and recombination in dye-sensitized solar cells studied by impedance spectroscopy. *Sol. Energy Mater. Sol. Cells* **2005**, *87*, 117−131.
(32) Morales-Guio, C. G.; Tilley, S. D.; Vrubel, H.; Grätzel, M.; Hu, X. Hydrogen evolution from a copper(I) oxide photocathode coated with an amorphous molybdenum sulphide catalyst. *Nat. Commun.* **2014**, *5*, 3059, DOI: 10.1038/ncomms4059.
(33) Prévot, M. S.; Sivula, K. Photoelectrochemical tandem cells for solar water splitting. *J. Phys. Chem. C* **2013**, *117*, 17879−17893.
(34) Paracchino, A.; Laporte, V.; Sivula, K.; Grätzel, M.; Thimsen, E. Highly active oxide photocathode for photoelectrochemical water reduction. *Nat. Mater.* **2011**, *10*, 456−461.
(35) Tilley, S. D.; Schreier, M.; Azevedo, J.; Stefik, M.; Grätzel, M. Ruthenium oxide hydrogen evolution catalysis on composite cuprous oxide water-splitting photocathodes. *Adv. Funct. Mater.* **2014**, *24*, 303−311.
(36) Benck, J. D.; Chen, Z. B.; Kuritzky, L. Y.; Forman, A. J.; Jaramillo, T. F. Amorphous molybdenum sulfide catalysts for electrochemical hydrogen production: Insights into the origin of their catalytic activity. *ACS Catal.* **2012**, *2*, 1916−1923.
(37) Laursen, A. B.; Vesborg, P. C. K.; Chorkendorff, I. A high-porosity carbon molybdenum sulphide composite with enhanced electrochemical hydrogen evolution and stability. *Chem. Commun.* **2013**, *49*, 4965−4967.
(38) Hsu, C.-L.; Chang, Y.-H.; Chen, T.-Y.; Tseng, C.-C.; Wei, K.-H.; Li, L.-J. Enhancing the electrocatalytic water splitting efficiency for amorphous MoS_x. *Int. J. Hydrogen Energy* **2014**, *39*, 4788−4793.
(39) Chang, Y.-H.; Lin, C.-T.; Chen, T.-Y.; Hsu, C.-L.; Lee, Y.-H.; Zhang, W.; Wei, K.-H.; Li, L.-J. Highly efficient electrocatalytic hydrogen production by MoS_x grown on graphene-protected 3D Ni foams. *Adv. Mater.* **2013**, *25*, 756−760.
(40) Chang, Y.-H.; Wu, F.-Y.; Chen, T.-Y.; Hsu, C.-L.; Chen, C.-H.; Wiryo, F.; Wei, K.-H.; Chiang, C.-Y.; Li, L.-J. Three-dimensional molybdenum sulfide sponges for electrocatalytic water splitting. *Small* **2014**, *10*, 895−900.
(41) Sun, Y. J.; Liu, C.; Grauer, D. C.; Yano, J. K.; Long, J. R.; Yang, P. D.; Chang, C. J. Electrodeposited cobalt-sulfide catalyst for electrochemical and photoelectrochemical hydrogen generation from water. *J. Am. Chem. Soc.* **2013**, *135*, 17699−17702.
(42) Tran, P. D.; Chiam, S. Y.; Boix, P. P.; Ren, Y.; Pramana, S. S.; Fize, J.; Artero, V.; Barber, J. Novel cobalt/nickel−tungsten−sulfide catalysts for electrocatalytic hydrogen generation from water. *Energy Environ. Sci.* **2013**, *6*, 2452−2459.
(43) Wang, T.; Zhuo, J.; Du, K.; Chen, B.; Zhu, Z.; Shao, Y.; Li, M. Electrochemically fabricated polypyrrole and MoS_x copolymer films as a highly active hydrogen evolution electrocatalyst. *Adv. Mater.* **2014**, *26*, 3761−3766.
(44) Seger, B.; Laursen, A. B.; Vesborg, P. C. K.; Pedersen, T.; Hansen, O.; Dahl, S.; Chorkendorff, I. Hydrogen production using a molybdenum sulfide catalyst on a titanium-protected n^+p-silicon photocathode. *Angew. Chem., Int. Ed.* **2012**, *51*, 9128−9131.
(45) Laursen, A. B.; Pedersen, T.; Malacrida, P.; Seger, B.; Hansen, O.; Vesborg, P. C. K.; Chorkendorff, I. MoS_2—An integrated protective and active layer on n^+p-Si for solar H_2 evolution. *Phys. Chem. Chem. Phys.* **2013**, *15*, 20000−20004.
(46) Tran, P. D.; Pramana, S. S.; Kale, V. S.; Nguyen, M.; Chiam, S. Y.; Batabyal, S. K.; Wong, L. H.; Barber, J.; Loo, J. Novel assembly of an MoS_2 electrocatalyst onto a silicon nanowire array electrode to construct a photocathode composed of elements abundant on the earth for hydrogen generation. *Chem.—Eur. J.* **2012**, *18*, 13994−13999.
(47) Bourgeteau, T.; Tondelier, D.; Geffroy, B.; Brisse, R.; Laberty-Robert, C.; Campidelli, S.; de Bettignies, R.; Artero, V.; Palacin, S.; Jousselme, B. A H_2-evolving photocathode based on direct sensitization of MoS_3 with an organic photovoltaic cell. *Energy Environ. Sci.* **2013**, *6*, 2706−2713.
(48) Tang, M. L.; Grauer, D. C.; Lassalle-Kaiser, B.; Yachandra, V. K.; Amirav, L.; Long, J. R.; Yano, J.; Alivisatos, A. P. Structural and electronic study of an amorphous MoS_3 hydrogen-generation catalyst on a quantum-controlled photosensitizer. *Angew. Chem., Int. Ed.* **2011**, *50*, 10203−10207.